Federal State Autonomous Educational Institution of Higher Education

National Research University Higher School of Economics

Unpublished manuscript

Chigarev Vladimir Gennadyevich

On chaotic attractors and repellers in systems with a compact phase space

SUMMARY OF THE THESIS

for the degree of Candidate of Science (Ph.D.) in Applied Mathematics

Scientific adviser:
Doctor of Science in Applied Mathematics, Professor
Kazakov Alexey Olegovich

Moscow – 2024

The dissertation work was carried out at the National Research University «Higher School of Economics».

Supervisor: Doctor of Science in Applied Mathematics, Professor Kazakov Alexey Olegovich

1 Introduction

Relevance. The study of attractors and repellers occupies a central place in problems of nonlinear dynamics. There are many different definitions of these objects, suitable for certain cases. As a rule, an attractor is understood as some compact subset of the phase space of a dynamical system, all trajectories from some neighborhood of which (absorbing region) tend to it over time. If the phase space of a system is compact (for example, a multidimensional torus in the case of phase dynamics, or a sphere in the case of torque oscillators), it is also possible to consider the dynamics of that system back in time and define a repeller as an attractor for the system in backward time.

As a rule, an isolated attractor and repeller do not intersect, but these two sets can collide and merge into one. The resulting set may turn out to be topologically conservative - when the attractor and repeller, as sets, coincide with the entire phase space. But it is also possible that the attractor and the repeller intersect, but do not coincide. In the second case, we get mixed dynamics - the third type of chaos (along with conservative and dissipative), the theory of which was laid down quite recently in the works of Gonchenko and Turaev. This theory is currently being actively developed. The creation of methods for studying systems with intersecting attractor and repeller, as well as effectively verifiable criteria that make it possible to distinguish mixed dynamics from the other two types of chaos, is one of the most pressing problems in nonlinear dynamics. On the other hand, it is important to note that in most modern works devoted to the study of mixed dynamics, the attractor and repeller were considered only as sets, while the issue of distribution of invariant measures on these sets was ignored.

This dissertation is devoted to the study of systems with compact phase space that demonstrate the intersection of chaotic attractors and repellers. A number of new results have been obtained in this direction. When studying the phenomenon of intersection of these two sets, it was proposed to consider not only the topology of these sets, but also the distribution of invariant measures on them, which made it possible to resolve a number of paradoxes associated with the discrepancy between the theory of mixed dynamics and the results of numerical experiments.

In Chapter 1, a method is proposed that allows, for conservative diffeomorphisms defined on a compact manifold, to construct dissipative perturbations for which inverse mappings are easily determined. Using this method, based on the Anosov mapping of a two-dimensional torus and the standard Chirikov mapping, two model examples were constructed. In the first example, adding dissipation results in topologically conservative chaos, although visually the attractor and repeller do not coincide; an explanation for this phenomenon is given. In the second case, when adding dissipation, we immediately get mixed dynamics, since due to the non-hyperbolicity of the mapping, the attractor cannot completely coincide with the repeller. In both cases, a new method for studying physical invariant measures is proposed based on

calculating the distances between physical measures for an attractor and a repeller. The method is used to study the limits of applicability of the linear response theory, including for the case of large external influences on the system.

Chapter 2 of the dissertation work is devoted to the study of the chaotic set resulting from the collision of a one-dimensional hyperbolic attractor with a one-dimensional hyperbolic repeller on a three-dimensional torus. Hyperbolic chaotic sets are ideal objects with good dynamic and statistical properties. There are many known mechanisms for the destruction of hyperbolicity. The dissertation proposed a new mechanism associated with the emergence of heterodimensional dynamics at the collision boundary of a hyperbolic attractor and a repeller. Such dynamics is characterized by the presence of trajectories inside a chaotic set with different numbers of positive Lyapunov exponents. In particular, when periodic trajectories inside a chaotic set have a different number of stable and unstable directions. It is noteworthy that conclusions about the stability of such a situation can be drawn on the basis of identifying the so-called heterodimensional cycles - trajectories connecting periodic trajectories with different dimensions of stable and unstable manifolds. The dissertation proposed a method for finding and constructing the corresponding cycles.

The relevance of the results of the work presented in Chapter 2 is due to two factors. First, a new phenomenon is discovered and explained - the collision of non-trivial hyperbolic attractors and repellers; the existence of heterodimensional dynamics after such a collision was established, and numerical methods for its detection were proposed. The results obtained make a significant contribution to the theory of multidimensional chaos. Secondly, these results also have an applied character and can be applied to phase synchronization problems. For example, the collision of a chaotic attractor and a repeller naturally arises when the chaotic phase synchronization is destroyed.

As part of the work on the dissertation, a software package was developed that makes it possible to carry out numerical studies of chaotic dynamics in systems with compact phase space. In particular, within the framework of the software package, such methods for studying systems with intersecting attractor and repeller have been implemented, such as calculating the Kantorovich-Rubinstein-Wasserstein distance, the mutual dimensions of Renyi, Kullback-Leibler and the spectrum of singularities between these two sets, the construction of heterodimensional cycles for a given pair of saddle periodic trajectories, dragging bifurcation curves by parameters, calculating various types of Lyapunov exponents, etc.

Degree of development. For the first time, the intersection of a chaotic attractor and a chaotic repeller in a numerical experiment was discovered in the work of Pikovsky-Topaj [1] in chains of coupled rotators. Together with theoretical studies by Gonchenko, Delchamps, Lamb, Stenkin, Thomas, Turaev, Shilnikov[2, 3, 4] of the irreducible and inseparable coexistence of attractors and repellers near certain types of homoclinic tangents, these studies formed the basis for the creation of Gonchenko and Turaev citegonchenko2016reversible, gonchenko2017three theory of mixed dynamics - the third type of chaos, characterized by the intersection, but not the coincidence, of attractor and repeller.

To date, mixed dynamics have been discovered in many systems from applications: in nonholonomic systems [7, 8, 9, 10, 11], in hydrodynamic models [12], in models of neuron-like connected elements [13, 14, 15] and others. Bifurcation scenarios for the occurrence of this phenomenon [16, 17, 12] have been proposed, numerical methods have been developed for

identifying mixed dynamics in the space of system parameters [18, 13, 14, 15], criteria for the emergence of mixed dynamics have been constructed [4, 9, 19]. However, in all these works the emphasis was on studying the topology of the intersecting attractor and repeller. At the same time, issues related to the structure of an invariant measure on attractors and repellers, namely the measure observed in systems during the numerical construction of these two sets, were avoided.

Chapter 1 of the dissertation pays special attention to these issues. A new effective method is proposed that allows one to quantitatively determine the distinguishability of invariant measures of an attractor and a repeller. The essence of this method is to calculate the Kantorovich-Rubinstein-Wasserstein distance between two measures, respectively, on the attractor and on the repeller. This method was previously used to compare two attractors taken at different values of the system parameters [20]. For intersecting attractor and repeller, this method was used for the first time in the work of the dissertation author. Also in Chapter 1, based on the theory of fractal dimensions, methods have been developed that make it possible to determine such characteristics of the intersecting attractor and repeller as relative dimensions and spectra of mutual singularity. In addition, based on the perturbation of the simplest mappings using the Möbius transform, a method for constructing simple model mappings of a two-dimensional torus is proposed, demonstrating the intersections of an attractor and a repeller with a non-zero dissipation parameter. The effectiveness of the method is demonstrated on such model mappings, as well as on more complex examples.

Chapter 2 of the thesis examines the phenomenon of collision of hyperbolic attractor and repeller in a mapping defined on a three-dimensional torus. In the works of Gonchenko, Kazakov, Turaev [16, 17, 12] it was shown that such a collision can lead to the emergence of mixed dynamics. The bifurcation mechanisms of the transition from separated attractor and repeller to mixed dynamics through the collision of these two sets were also explained. For three-dimensional displays, a similar phenomenon was discovered in the work of Pikovsky, Osipov, Rezenblum, Zaks[21]. The dissertation author gave an explanation of this phenomenon in the language of the theory of bifurcations. It is shown that immediately after the collision of the attractor and the repeller, one chaotic set arises, coinciding with the entire three-dimensional torus and containing trajectories with different dimensions of unstable manifolds. By identifying heterodimensional cycles immediately after the collision of the attractor and the repeller, conclusions were drawn about the stability of the resulting chaotic set.

The theory of heterodimensional cycles - heteroclinic contours connecting periodic trajectories with different dimensions of stable and unstable manifolds was founded in the work of Bonatti and Diaz [22]. The work of Abraham and Smale [23] proposed one of the first scenarios for the violation of hyperbolicity associated with the emergence of heterodimensional cycles. The irreducibility of non-transversal intersections of invariant manifolds in such cycles was established and studied by Diaz and his colleagues [24, 25, 26]. The mathematical theory for mappings with heterodimensional cycles of coindex one (when the difference between the unstable manifolds of a pair of saddle orbits connected by these cycles is equal to unity) was developed by Bonatti and Diaz [22, 27], where the authors proved the C^1-stability of heterodimensional cycles . A general version of this result with higher smoothness was recently obtained by Li and Turaev [28]. The results of the work [28] guarantee the existence of heterodimensional dynamics in a two-parameter family of diffeomorphisms, giving a suitable

bifurcation development of the heterodimensional cycle.

In conclusion of the review, we note that there are alternative approaches that allow one to draw a conclusion about the robustness (stability to disturbances) of heterodimensional dynamics. For example, by identifying a blender - a compact invariant set for which topologically "thin" sets inevitably intersect, guaranteeing the robustness of heterodimensional dynamics. Such methods were developed in the works of Krauskopf, Osinga and their co-authors[29, 30, 31]. However, these methods are very complex and time-consuming. In the thesis, the conclusion about the robustness of heterodimensional dynamics after a collision between an attractor and a repeller is made on the basis of finding only four trajectories that form a heterodimensional cycle.

Goals and objectives of the study. The goal of the thesis is to develop new methods for studying the chaotic dynamics of diffeomorphisms defined on a compact manifold. Using these methods, study the features of the chaotic dynamics of mappings of a two-dimensional and three-dimensional torus.

To achieve these goals, the following tasks were considered:

- construction of model mappings demonstrating the formation of the intersection of an attractor and a repeller when changing a parameter;
- study of the properties of physical invariant measures based on calculating the Kantorovich-Rubinstein-Wasserstein distance between the physical measure on the attractor and the physical measure on the repeller;
- study of mutual dimensions for intersecting attractor and repeller;
- description of collision mechanisms of nontrivial hyperbolic attractor and repeller for diffeomorphisms defined on a three-dimensional torus;
- creation of methods for identifying and constructing heterodimensional cycles;
- development of a software package that implements the methods listed above.

Research methods. To solve the problems posed in the dissertation work, qualitative, analytical and numerical methods of the theory of dynamic systems were used. Analytical methods were used to construct dissipative perturbations of area-preserving mappings, as well as to find some bifurcation curves. Qualitative methods of bifurcation theory were used to develop a collision scenario between a hyperbolic attractor and a repeller, as well as to develop a method for constructing heterodimensional cycles. Numerical methods were used to calculate the Kantorovich-Rubinstein-Wasserstein distance, relative dimension, and singularity spectrum for an intersecting attractor and repeller. In this case, to calculate the Kantorovich-Rubinstein-Wasserstein distance, the software packages «PyEMD: Earth mover's distance for Python» and «CLP: COIN linear program code» were used, and the calculations of relative dimensions and the singularity spectrum were carried out using our own software. Numerical methods are implemented in C language++; Python language was used to visualize the results.

Theoretical and practical significance. The theoretical significance of the dissertation work lies in the development of new approaches and methods for studying dynamic chaos characterized by the intersection of an attractor and a repeller, as well as in the creation of

a new method for constructing dissipative perturbations for conservative mappings defined on compact manifolds. The solution to these problems seems to be a significant advance for the theory of dynamic chaos.

The practical significance of the results obtained is determined by the following three aspects. The methods for comparing chaotic sets, in particular attractor and repeller, developed in Chapter 1 are universal in nature and applicable to a wide range of systems (including experimental observations). Usually, when studying the dependence of dynamics on parameters or on external influences, the emphasis is on bifurcation analysis, which makes it possible to track qualitative changes in dynamics. Our method allows us to characterize the difference between the dynamic indicators of qualitatively identical modes. This is especially important for describing effects at small perturbations, for which one can expect a linear dependence of the distances between modes depending on the magnitude of the perturbation. Our results show that for a certain class of systems the linear dependence is preserved, including at large disturbance values, which allows us to conclude that the dynamics are robust with respect to external influences, including large ones. In addition, according to citation statistics in the "google.scholar" system, the developed methods were used in more than 20 papers devoted to the study of systems from a variety of applications (neurodynamics models, the problem of encoding audio information, models of rigid body motion, etc.) , which indicates the high practical significance of the results obtained.

Secondly, the transition to heterodimensional dynamics described in Chapter 2 is directly applicable to a number of applied problems. Our model generalizes the standard saddle-node bifurcation to the case of chaotic influence. The standard saddle-node bifurcation describes the transition from equilibrium to motion in many physical systems, such as the synchronization of oscillators, the current-voltage characteristic of the Josephson junction, and the mobility of particles in a periodic potential. In all these examples, in the presence of chaotic influence (both with a chaotic external force for Josephson contacts, and with internal chaotic dynamics in the presence of additional degrees of freedom for oscillators and active mobile particles), the transition proceeds according to the scenario described in Chapter 2. Thus, the study of the mechanisms The collision of attractor and repeller in our display allows us to understand the mechanisms of destruction of chaotic phase synchronization in ensembles of interacting elements. We also note that according to citation statistics in the "google.scholar" system, the theory presented in Chapter 2 has found application in studies of the mobility of active particles.

Thirdly, in the process of working on the dissertation, a software package was developed, within which a number of methods for studying attractors and repellers were implemented. This software package was used to study the models discussed in the dissertation. However, its functionality allows the study of broader classes of dynamical systems that exhibit collision and intersection of attractors and repellers.

Results submitted for defense.

1. New methods for studying the chaotic dynamics of diffeomorphisms defined on a compact manifold.

   Based on the calculation of various types of distances between a numerically determined physical invariant measure for a system in direct time and the corresponding measure for

the same system in reverse time, methods have been developed that make it possible to determine the limits of applicability of the linear response theory, in particular, to study the case of a large external influence on the system, and also explore the reversibility properties of the system; a new method for checking the presence/absence of non-uniform hyperbolicity is proposed.

2. New scenario for the collision of a chaotic attractor with a chaotic repeller for maps defined on a three-dimensional torus.

   Using the example of a three-dimensional map, which is the skew product of a two-dimensional Anosov diffeomorphism and a one-dimensional Möbius map, it is shown that a hyperbolic attractor can collide with a hyperbolic repeller as a result of a saddle-saddle bifurcation, when one of the saddle periodic points belonging to the attractor merges with a saddle periodic point, belonging to the repeller. It is shown how, as a result of an infinite cascade of such bifurcations, the physical measures on the attractor and repeller become indistinguishable. A procedure for constructing a heterodimensional cycle immediately after the collision of a hyperbolic attractor and a hyperbolic repeller has been proposed and tested.

3. A software package for the study of reversible and dissipative systems.

   A software package has been developed that allows calculating the Kantorovich-Rubinshtein-Wasserstein distance, mutual dimensions, singularity spectrum, spectrum of short Lyapunov exponents for intersecting attractors and repellers, as well as finding heterodimensional cycles.

Novelty and reliability. The results described in the dissertation work are new. They are in good agreement with existing theoretical concepts and provisions. Numerical experiments are described in detail. Some of them were reproduced by the co-authors of the dissertation for verification. To calculate the Kantorovich-Rubinstein-Wasserstein distance, two different software packages were used, in both cases the results obtained were the same.

The results to be defended were published in three articles in the journal Chaos: An Interdisciplinary Journal of Nonlinear Science (Web of Science, Q1) - one of the leading journals on the theory of dynamic chaos and its applications.

Approbation of the obtained results. The main results of the dissertation were reported at the following international conferences and seminars:

1. Poster presentation *"Kantorovich-Rubinstein-Wasserstein distance between attractor and repeller"*, international conference «Shilnikov WorkShop 2020» December 17-18, 2020 Nizhny Novgorod

2. Poster presentation *"On the collision of a chaotic attractor with a chaotic repeller leading to the emergency of hyperchaotic orbits"*, international conference «Shilnikov WorkShop 2021» December 16-17, 2021 Nizhny Novgorod

3. Report *"Attractor-repeller collision and the heterodimensional dynamics"*, international conference «Shilnikov WorkShop 2022» December 19-20, 2022 Nizhny Novgorod

4. Report *"Metric similarity estimates between chaotic attractors and repellers"*, KROMSH 2020 Laspi-Batiliman.

5. Report *"Spectra of mutual singularities of overlapping attractor and repeller"*, KROMSH 2021 pos. Satera, Alushta.

6. Report *"Kantorovich-Rubinstein-Wasserstein distance between overlapping attractor and repeller"*, scientific seminar of the International Laboratory for Dynamic Systems and Applications, April 24, 2020. Nizhny Novgorod

7. Report *"Mutual singularities of an intersecting attractor and repeller"*, scientific seminar of the International Laboratory of Dynamic Systems and Applications, October 01, 2021 Nizhny Novgorod

8. Report *"Attractor-repeller collision and heterodimensional dynamics"*, scientific seminar of the International Laboratory for Dynamical Systems and Applications, January 18, 2023. Nizhny Novgorod

List of articles submitted for defense on the topic of the dissertation, indicating the personal contribution of the dissertation.

[1*] Chigarev V., Kazakov A., Pikovsky A. *Kantorovich-Rubinstein-Wasserstein distance between overlapping attractor and repeller*//Chaos: An Interdisciplinary Journal of Nonlinear Science **30** (2020), C. 073114

https://doi.org/10.1063/5.0007230

(Principal co-author. A method for constructing dissipative perturbations for conservative mappings defined on a torus was proposed. Numerical experiments were carried out to calculate the Kantorovich-Rubinshtein-Wasserstein distance for intersecting attractors and repellers.)

[2*] Chigarev V., Kazakov A., Pikovsky A. *Mutual singularities of overlapping attractor and repeller*//Chaos: An Interdisciplinary Journal of Nonlinear Science **31** (2021), C. 083127

https://doi.org/10.1063/5.0056891

(Principal co-author. Numerical experiments were carried out to calculate the relative dimensions and spectra of the mutual singularity of the attractor and repeller.)

[3*] Chigarev V., Kazakov A., Pikovsky A. *Attractor–repeller collision and the heterodimensional dynamics*//Chaos: An Interdisciplinary Journal of Nonlinear Science **33** (2023), C. 063113

https://doi.org/10.1063/5.0144672

(Principal co-author. The scenario of collision of hyperbolic attractor and repeller is described, a method for constructing heterodimensional cycles is proposed, all numerical experiments are performed.)

2 Summary of the work. Main results

The main results of the dissertation work are contained in three chapters:

- Kantorovich-Rubinshtein-Wasserstein distance, relative dimensions and mutual singularities of the intersecting attractor and repeller;
- collision of a chaotic attractor with a chaotic repeller in mappings defined on a three-dimensional torus and heterodimensional dynamics;
- numerical methods and software package.

2.1 Kantorovich-Rubinstein-Wasserstein distance, relative dimensions and mutual singularities of the intersecting attractor and repeller

In Chapter 1, for systems exhibiting the intersection of a chaotic attractor and a chaotic repeller, we quantify the distinguishability of these two sets. At the same time, we bypass questions related to the topology and structure of these two sets[1] are devoted to these issues, focusing more on questions related to the distribution of invariant measures on the attractor and repeller, respectively. Moreover, speaking about attractors and repellers, we will mean the invariant measure for the system in direct and reverse time, respectively, unless otherwise discussed separately.

First, we introduce 4 basic models: three maps defined on a 2D torus and a system of differential equations defined on a 3D torus.

The first mapping is the Anosov mapping A:

$$\begin{aligned} x_{n+1} &= 2x_n + y_n \pmod 1 , \\ y_{n+1} &= x_n + y_n \pmod 1 . \end{aligned} \tag{1}$$

This is a striking example of conservative hyperbolic chaos [32], see Fig. 1a, demonstrating that the stable and unstable manifolds of the saddle fixed point $O(0,0)$ intersect transversally.

The second mapping is the standard Chirikov mapping C

$$\begin{aligned} x_{n+1} &= x_n + K\sin(2\pi y_n) \pmod 1 , \\ y_{n+1} &= y_n + x_{n+1} \pmod 1 , \end{aligned} \tag{2}$$

which is the prototype of Hamiltonian dynamics with separated phase space [33]. For small values of the parameter K the dynamics is close to integrable, while for $K \gg 1$ it is predominantly chaotic. The chaos here is not hyperbolic, since stable and unstable manifolds of periodic saddle points can have tangency, see fig. 1b. Thus, the existence of elliptic periodic points [34] and stability islands around them is not ruled out. In practice, for sufficiently large values of the parameter K, it is difficult to detect such islands. Here we take $K = 14/(2\pi)$, that is, we are just considering the case in which stability islands do not appear.

[1] For example, the following works [5, 16, 6, 9].

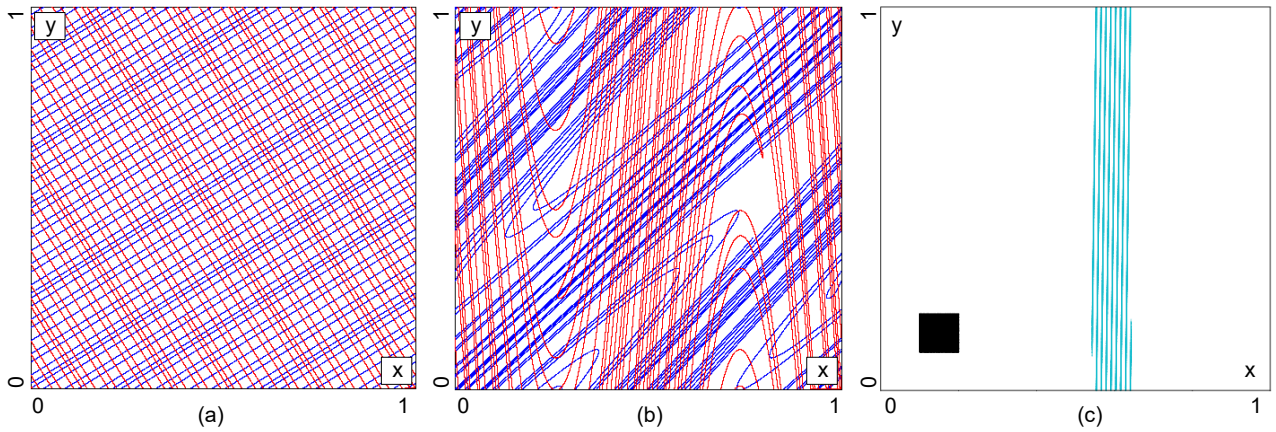

Рис. 1: Stable (colored in red) and unstable (colored in blue) invariant manifolds of the saddle fixed point $(0, 0)$ (a) for the Anosov mapping (1) and (b) for the standard Chirikov mapping (2) with $K = 14/(2\pi)$; (c) the image of the square $([0.1, 0.2] \times [0.1, 0.2])$ densely filled with initial points after the 80th iteration of the mapping (3).

The third mapping is a linear oblique shift along the rotation of the circle, S

$$\begin{aligned} x_{n+1} &= x_n + y_n \pmod 1 , \\ y_{n+1} &= y_n + \omega \pmod 1 . \end{aligned} \tag{3}$$

This mapping is not chaotic, it has two zero Lyapunov exponents. It is known that for irrational values of the rotation parameter ω this mapping is ergodic [35]. Below we fix this parameter in a value equal to the inverse of the golden ratio ($\omega = (\sqrt{5} - 1)/2$). To illustrate its ergodicity, Fig. 1c shows the nth iteration of a small rectangle ($[0.1, 0.2] \times [0.1, 0.2]$) densely filled with starting points. For $n \to \infty$ the image of this rectangle gives a set dense along the y axis. Figure 1c demonstrates this fact for $n = 80$.

In all mappings introduced above, the attractor coincides with the repeller. To «split» these sets, i.e. in order for the measure on the attractor to differ from the measure on the repeller, it is necessary to introduce dissipation, which destroys the phase volume conservation property and makes the Jacobian less than unity in some areas on the torus, and more in others. To do this, we use the Möbius mapping $M(\varepsilon, u, v)$ [36, 37]

$$e^{i2\pi(x_{n+1}-v)} = \frac{\varepsilon + e^{i2\pi(x_n-u)}}{\varepsilon e^{i2\pi(x_n-u)} + 1}. \tag{4}$$

This mapping is a mapping of the circle $x_n \to x_{n+1} \pmod 1$ depending on three parameters $0 \le u, v < 1$ and $-1 < \varepsilon < 1$. The ε parameter determines the degree of compression on the circle. For $\varepsilon = 0$ the Möbius map is a circle shift. For $\varepsilon \to 1$ it maps almost the entire circle to a small neighborhood of one point on it.

For the (4) mapping, it's easy to define an inverse mapping:

$$M^{-1}(\varepsilon, u, v) = M(-\varepsilon, v, u)$$

The action of the Möbius mapping for various values of the dissipation parameter ε ($u = v = 0$), as well as its inverse mapping, is illustrated in Fig. 2.

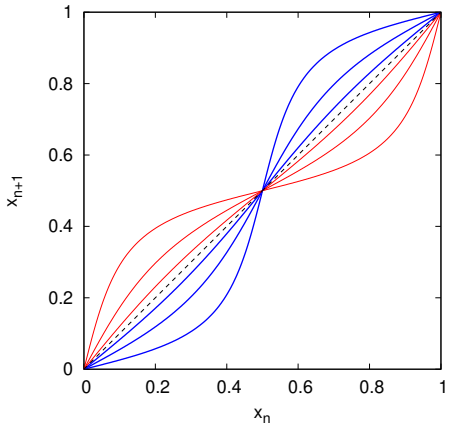

Рис. 2: Möbius mapping (blue lines) $M(\varepsilon, 0, 0)$ and inverse Möbius mapping $M^{-1}(-\varepsilon, 0, 0)$ (red lines) for three values of the dissipation parameter $\varepsilon = 0.1,\ 0.3,\ 0.6$.

To perturb the conservative mappings described above with the help of the Möbius mapping $M(\varepsilon, u, v)$ (4), we construct a composition of these mappings with a two-dimensional mapping of the form

$$\mathcal{M}_\varepsilon = \begin{pmatrix} M(\varepsilon, 0, 0) & 0 \\ 0 & 1 \end{pmatrix}. \tag{5}$$

We consider two types of such compositions: the simplest and the symmetrical. In the first case, we get mappings of the form:

$$\mathcal{A}: \ \mathcal{M}_\varepsilon A, \tag{6}$$

$$\mathcal{C}: \ \mathcal{M}_\varepsilon C, \tag{7}$$

$$\mathcal{S}: \ \mathcal{M}_\varepsilon S. \tag{8}$$

In the second case, we apply the mapping (5) to the mappings A, C and S in a symmetrical manner, preserving the symmetry with respect to forward and backward iterations in time:

$$\mathcal{AS}: \ \mathcal{M}_\varepsilon \ A \ \mathcal{M}_\varepsilon, \tag{9}$$

$$\mathcal{CS}: \ \mathcal{M}_\varepsilon \ C \ \mathcal{M}_\varepsilon, \tag{10}$$

$$\mathcal{SS}: \ \mathcal{M}_\varepsilon \ S \ \mathcal{M}_\varepsilon. \tag{11}$$

As a fourth model example, we consider an example of an intersecting attractor and repeller in a system with continuous time. We build our example on the three-dimensional torus $0 \le x_i < 1$, $i = 1, 2, 3$ as follows. First, we write a dynamical system that preserves the phase volume, similar to the three mappings described above:

$$\dot{x}_k = \sum_j (A_{kj} \cos 2\pi x_j + B_{kj} \sin 2\pi x_j + C_{kj} \cos 4\pi x_j + D_{kj} \sin 4\pi x_j) \ . \tag{12}$$

Here A_{kj}, B_{kj}, C_{kj} and D_{kj} are parameters. Next, we assume

$$A_{kk} = B_{kk} = D_{kk} = 0, \qquad C_{kk} = \varepsilon,$$

which allows you to control the phase volume divergence using the ε parameter. For $\varepsilon = 0$, the phase volume is preserved, and for $\varepsilon \neq 0$, the volumes are compressed in one part of the phase space, and stretched in the other. Next, we sorted through the values of the coefficients $A_{kj}, B_{kj}, C_{kj}, D_{kj}$ randomly from a uniform distribution on the interval $(-0.5, 0.5)$ until we found a set that gives chaotic dynamics in both forward and reverse time on a certain interval of the parameter ε $(0 \leq \varepsilon < 0.035)$.

All four proposed model examples (three mappings defined on a two-dimensional torus and a flow defined on a three-dimensional torus) have the following property in common:

- for $\varepsilon > 0$, the numerically constructed attractor intersects with the numerically constructed repeller, but these two sets are visually different and this difference cannot be eliminated by increasing the accuracy of attractor and repeller construction.

Further in the chapter, we introduce the concept of the Kantorovich-Rubinstein-Wasserstein (KRW) distance for a quantitative description of the degree of distinguishability of the numerically constructed attractor and repeller and successfully apply it to all four introduced models. The CRV distance characterizes the measure of proximity between two probability measures μ and ν. It is defined as the optimal solution to the transport problem according to Monge and Kantorovich, namely, as a transport protocol that minimizes the costs required to transport the mass from μ to ν. We assume that both measures are weighted sets of point measures (that is, their densities are sets of delta functions, see [20]):

$$\mu = \sum_{i=1}^{n_1} \alpha_i \delta_{x_i}, \qquad \nu = \sum_{j=1}^{n_2} \beta_j \delta_{y_j} \ .$$

Then any matrix $f_{ij} \geq 0$, $1 \leq i \leq n_1$, $1 \leq j \leq n_2$ satisfying the relations

$$\sum_i f_{ij} = \beta_j, \quad \sum_j f_{ij} = \alpha_i,$$

produces a possible transportation that transfers one measure to another. Optimal transportation should minimize the cost function determined according to «work done». The work performed, in turn, is equal to the multiplication of the transported mass f_{ij} by the distance $c_{ij} = ||x_i - y_j||_2$ between two points. Thus, the minimum cost function can be written as follows

$$W(\mu, \nu) = \min \sum_{i,j} f_{ij} c_{ij} \ .$$

We call this function the Kantorovich-Rubinshteion-Wasserstein distance between two measures μ and ν. Any metric can be used here as the distance c_{ij}. We use the Euclidean distance.

In the first part of Chapter 1, numerical experiments were carried out on the applicability of the KRF distance concept for assessing the degree of distinguishability of attractors and repellers to all four models under consideration: the experimental results for three model mappings are presented in Fig. 3. In all cases, it was found that the distance increases linearly with increasing dissipation parameter ε, through which the systems are perturbed from the

ideal case when the attractor exactly coincides with the repeller. Note that for intersecting attractor and repeller, this method was used for the first time in the work of the dissertation author.

The second part of Chapter 1 is devoted to the study of the fractal properties of the intersecting attractor and repeller. Here, studies of the relative dimensions of Rényi and the spectra of mutual singularity of these two sets are carried out, in the case when they have a common support. The results obtained show that the range of relative dimensions and mutual singularities grows with the growth of the dissipation parameter, as expected. It is also shown that the most convenient distinguishability characteristic between an attractor and a repeller, which best reflects the fractal properties of these two sets, is the Kullback-Leibler divergence (dimension). It is found that this dimension vanishes if the attractor and repeller coincide and grows quadratically with the dissipation parameter. In addition, it is shown that for all the examples considered, the relative dimensions and mutual singularities of the intersecting attractor and repeller can be derived quite accurately from the fractal properties of the attractor and repeller separately. Despite the fact that such a representation is theoretically substantiated only for orthogonal fractal measures, our calculations have shown that this approach gives very accurate results for non-orthogonal measures as well, moreover, both in the case of hyperbolic and non-hyperbolic mappings.

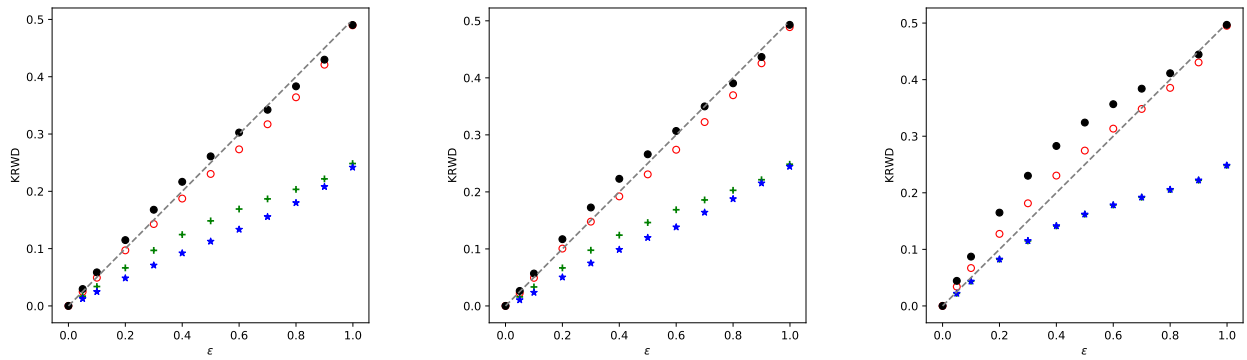

a) b) c)

Рис. 3: Results of calculating the Kantorovich-Rubinstein-Wasserstein distance for (a) Anosov-Möbius mapping (6), (b) Chirikov-Möbius (7) and (c) oblique shift mapping (8). Red circles indicate the distances between the attractor and the repeller, green pluses indicate the distances between the attractor and the uniform distribution, blue asterisks indicate the distances between the repellers and the uniform distribution (in Fig. (c) the asterisks overlap with the pluses). Black filled circles correspond to the sums of values marked with pluses and asterisks. The shaded lines have a slope of 0.5.

Next, we will carry out calculations of the KRW distance for the Anosov-Möbius map (6) and the Chirikov-Möbius map (7) on a more detailed grid in order to determine the limits of applicability of the linear response theory. Linear response theory is a technique that is used to analyze the behavior of a system under small disturbances by linearizing its dynamics around an equilibrium point. Graphs illustrating the results are presented in Fig. 4. From these graphs we draw conclusions:

- the distance of the RV increases linearly with respect to the parameter ε at small values of the parameter;

- the nearly linear growth also persists for large values of the parameter ε (up to $\varepsilon = 1$);
- the considered mappings are non-reversible;
- in the space of invariant measures, the Lebesgue measure lies close to the line connecting the measure on the attractor with the measure on the repeller;
- at $\varepsilon = 1$ the result is confirmed analytically;
- for the Chirikov-Möbius map (7) the dependence of the KRW on the parameter is non-smooth;

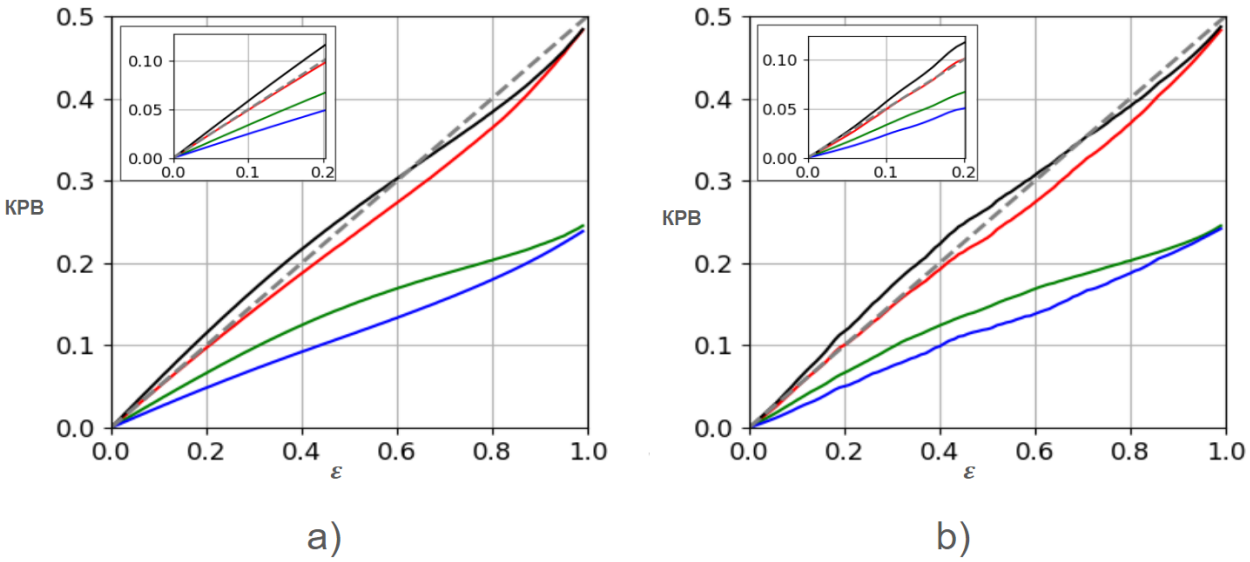

Рис. 4: Results of calculating the Kantorovich-Rubinstein-Wasserstein distance for (a) Anosov-Möbius mapping (6) and (b) Chirikov-Möbius (7) with a more detailed step. Red – distances between attractor and repeller, green – distances between attractor and Lebesgue measure, blue – distances between repeller and Lebesgue measure, black = green + blue, gray straight line has a slope of 0.5

The second part of Chapter 1 is devoted to the study of the fractal properties of the intersecting attractor and repeller. Here we carried out studies of the relative Renyi dimensions and the spectra of the mutual singularity of these two sets, in the case when they have a common carrier. The theory of generalized dimensions and spectra of singularities for a fractal measure is quite well developed and has proven itself in various applications. Let us recall its main elements for the sake of completeness. Consider the set U with a fractal measure. Covering the set with cells of size ϵ, we obtain a finite-dimensional approximation of the fractal measure with cell measures u_i (normalization requires $\sum_i u_i = 1$). Moving on to smaller partitions, the quantities $\tau(q;U)$ and the generalized dimensions $D(q;U)$ are determined according to

$$\tau(q;U) = \lim_{\epsilon\to 0} \frac{\ln \sum_i u_i^q}{\ln \epsilon}, \qquad D(q;U) = \frac{\tau(q;U)}{q-1} = \lim_{\epsilon\to 0} \frac{1}{q-1} \frac{\ln \sum_i u_i^q}{\ln \epsilon} . \tag{13}$$

Please note that the sum in (13) can be represented as an average over cells of a finite size. $\sum_i u_i^q = \langle u^{q-1} \rangle_U$. The most important are: Minkowski dimension $D(0;U)$ (gives the number of voids); information dimension $D(1;U)$ (gives the average crowding index); and the correlation dimension $D(2;U)$ (easily calculated by the Grassberger-Procaccia method [38]). Relative Renyi dimensions are defined as:

$$D^R(q;U||V) = \lim_{\epsilon\to 0} \frac{R(\epsilon,q;U||V)}{\ln\epsilon} = \lim_{\epsilon\to 0} \frac{1}{q-1} \frac{\ln \sum_i u_i^q v_i^{1-q}}{\ln\epsilon} = \lim_{\epsilon\to 0} \frac{1}{q-1} \frac{\ln \left\langle \left(\frac{u_i}{v_i}\right)^{q-1} \right\rangle_U}{\ln\epsilon}. \quad (14)$$

на основе формулы дивергенции Реньи

$$R(\epsilon,q;U||V) = \frac{1}{q-1} \ln \sum_i u_i^q v_i^{1-q} = \frac{1}{q-1} \ln \left\langle \left(\frac{u_i}{v_i}\right)^{q-1} \right\rangle_U . \quad (15)$$

where U and V are two fractal measures *having a common carrier* with corresponding values in ϵ-cells u_i and v_i, Here the index at the averaging sign indicates that averaging is performed according to the measure U.

In the ideal case, the fractal directions of the sets U and V are strictly orthogonal. In addition, since the above concepts apply to sets with common support, we consider two measures that have Minkowski dimension equal to the full dimension of the phase space (in our case 2). In other words, there are no voids in these sets (which is typical for standard Cantor sets), but their measures are multifractals. Therefore, we will assume that on the unit square the measure U is fractal along the x axis (and we denote the projection of the measure onto the x axis as μ) and uniform along the y axis. The measure V is assumed to be fractal along the y axis (we denote the projection onto the y axis as ν) and uniform along the x axis. The measures of a two-dimensional cell with indices (i,j) of size ε are equal to $u_{ij} = \mu_i\varepsilon$ and $v_{ij} = \nu_j\varepsilon$.

Fractal dimensions of measures are obtained by substituting these expressions into (13):

$$\begin{aligned} \tau(q;U) &= \lim_{\varepsilon\to 0} \frac{\ln \sum_i \mu_i^q + (q-1)\ln\varepsilon}{\ln\varepsilon} = \tau(q;\mu) + q - 1 , \qquad D(q;U) = D(q;\mu) + 1 , \\ \tau(p;V) &= \lim_{\varepsilon\to 0} \frac{\ln \sum_j \nu_j^p + (p-1)\ln\varepsilon}{\ln\varepsilon} = \tau(p;\nu) + p - 1 , \qquad D(p;V) = D(p;\nu) + 1 . \end{aligned} \quad (16)$$

Let us emphasize here that since the support of two measures is the entire square, $D(0;\mu) = D(0;\nu) = 1$.

Similar calculations of the relative Renyi dimension give

$$D^R(q;U||V) = D(q;\mu) + \frac{qD(1-q;\nu) - 1}{1-q} = D(q;U) + \frac{qD(1-q;V) - 2}{1-q} . \quad (17)$$

The obtained results of calculations of relative Renyi dimensions (Fig. 5) show that the range of relative dimensions increases with increasing dissipation parameter, as expected. It is also shown that the most convenient characteristic of distinguishability between an attractor and a repeller, which best reflects the fractal properties of these two sets, is the Kullback-Leibler divergence (dimension). It has been established that this dimension goes to zero if the attractor and repeller coincide, and increases quadratically with the dissipation parameter. Additionally,

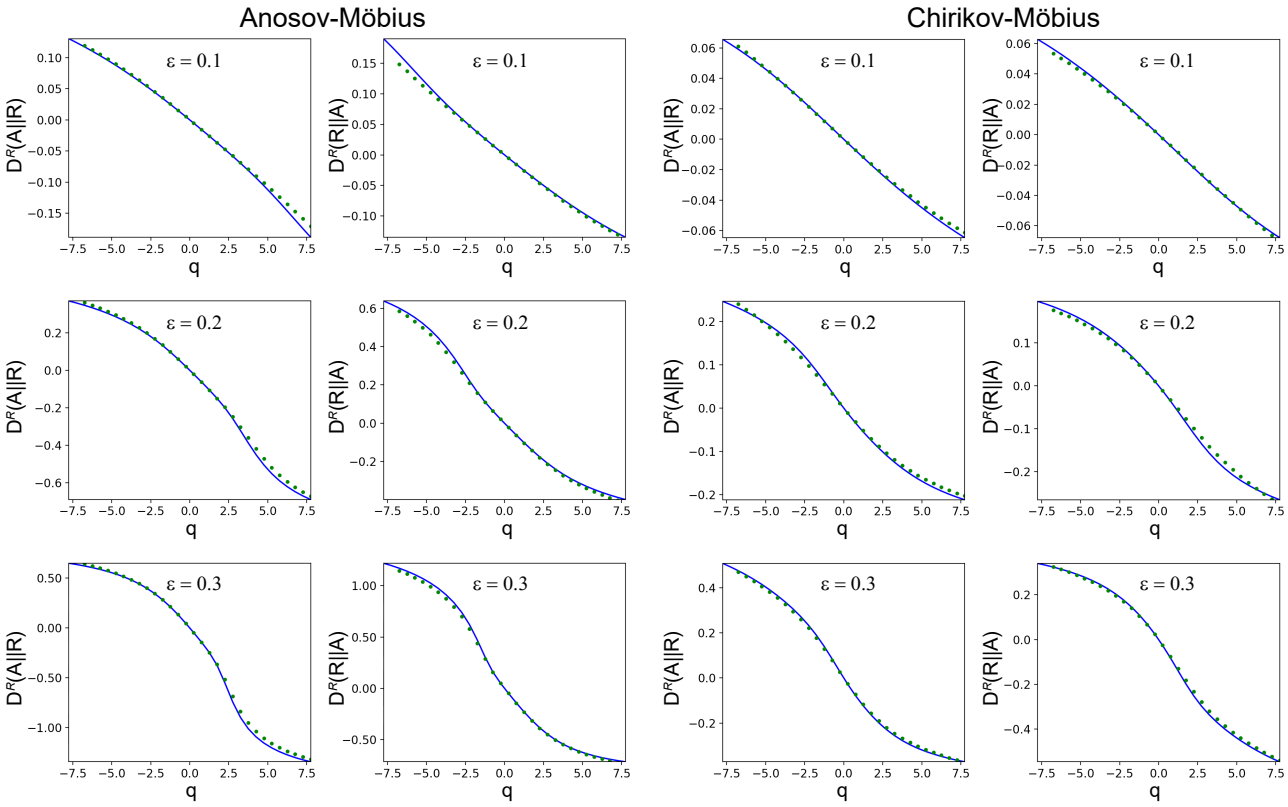

Рис. 5: Relative Rényi dimensions for the Anosov-Möbius map (6) (two columns on the left) and the Chirikov-Möbius map (7) (two columns on the right); odd columns: $D^R(q; A||R)$, even columns: $D^R(q; R||A)$. The rows from top to bottom correspond to the values of the dissipation parameter in the Möbius map $\varepsilon = 0.1,\ 0.2,\ 0.3$. The blue curves correspond to the direct calculation of the mutual dimensions between the attractor and the repeller; green circles are the values of partial dimensions obtained using the orthogonality relation (17). It can be seen that this relationship works well in all cases. Note that in all cases $D^R(q = 0) = 0$, as it should be for two measures having the same support (see property 6 when discussing Rényi dimensions).

it is shown that for all considered examples, the relative dimensions of the intersecting attractor and repeller can be quite accurately derived from the fractal properties of the attractor and repeller separately. Despite the fact that such a representation is theoretically justified only for orthogonal fractal measures, our calculations have shown that this approach also gives very accurate results for non-orthoganal measures, moreover, both in the case of hyperbolic and non-hyperbolic mappings.

2.2 Collisions between an attractor and a repeller and heteroexchange dynamics

Chapter 2 explores the phenomenon of collision between a hyperbolic attractor and a hyperbolic repeller in a mapping defined on a three-dimensional torus. As a model system, here

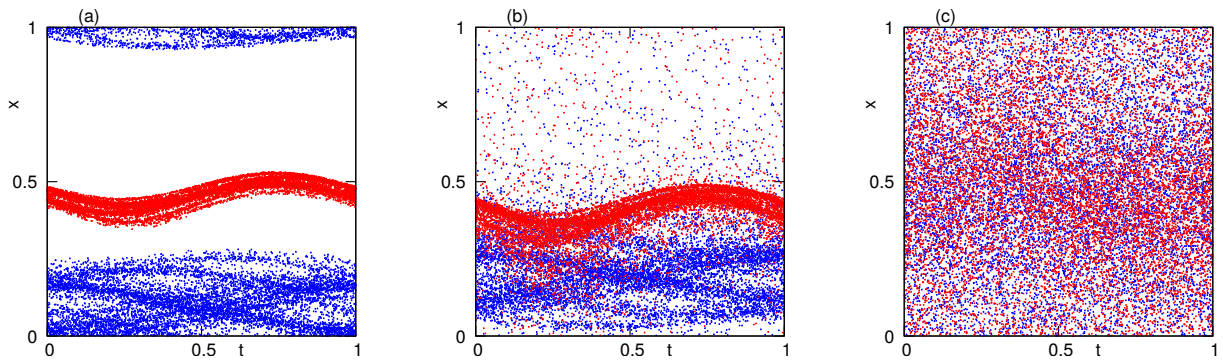

Рис. 6: Projections of the attractor (blue dots) and repeller (red dots) for $\varepsilon = 0.4$, $\alpha = 0$ and $\mu = 0.1$. (a) $c = 0.05$, attractor and repeller are separated; (b) $c = 0.1$, the attractor and repeller intersect, but the corresponding invariant measures are completely different; (c) $c = 0.4$, the measures of the intersecting attractor and repeller are very similar.

we consider a chaotically controlled mapping of a circle

$$t_{n+1} = 2t_n + s_n \pmod 1\,, \tag{18a}$$

$$s_{n+1} = t_n + s_n \pmod 1\,, \tag{18b}$$

$$x_{n+1} = x_n + c + \mu \sin(2\pi t_n + \alpha) - \frac{1}{\pi}\arctan\left(\frac{\varepsilon \sin 2\pi x_n}{1 + \varepsilon\cos 2\pi x_n}\right) \pmod 1. \tag{18c}$$

Here the equations (18a)–(18b) describe the Anosov control map, and the equation (18c) is the Möbius control map. Note that systems like (18) arise in the context of chaotic phase synchronization problems [21], when periodic excitations of a chaotic attractor with a well-defined phase variable are studied. In this context, the (18) system and its parameters can be interpreted as follows. The Anosov mapping (18a)–(18b) describes the chaos of the amplitude variables of the attractor, and the variable x in the equation 18c corresponds to the phase. The μ parameter describes the «internal link» between amplitude and phase; it determines phase diffusion and is related to the level of coherence of free chaotic oscillations (large values of μ correspond to stronger phase diffusion, small values of μ mean almost regular phase rotations). The features of this internal connection depend on the additional phase shift α. The terms c and ε describe the effect of an external periodic force on a chaotic attractor, their meaning is the same as in the context of the reduction of the mapping on a circle for forced periodic oscillations: c is approximately proportional to the detuning of the phase mismatch frequencies, and ε describes the amount of arousal.

Figure 6 shows a chaotic attractor and a chaotic repeller in the (18) system. To construct them, we numerically built sufficiently long trajectories of some initial point in direct (for constructing an attractor) and reverse (for constructing a repeller) time, discarding the initial points corresponding to transient processes. These trajectories give insight into the invariant measures of the attractor and repeller. In the situation shown in Fig. 6a, these sets are separated: the attractor lies in some absorbing region, while the repeller serves as a chaotic saddle in direct

time, near which a long-lived transient dynamics is observed [39]. When time is reversed in the mapping, these two sets change roles. Figures 6b and 6c show cases of intersecting attractor and repeller. In this case, both of these sets are dense in the entire phase space (on the entire three-dimensional torus). However, the invariant measures of the attractor and repeller in the case of fig. 6b are completely different, and in the case of fig. 6c, these measures almost coincide. The transition from separated attractor and repeller (fig. 6a) to intersecting these sets (fig. 6b,c) is called *attractor-repeller collision* [21].

In the first part of Chapter 2, we describe the bifurcations that accompany this collision. For the map (18), the corresponding bifurcations lend themselves very well to investigation, thanks to the special properties of the Möbius map. Any iteration of it is again a Möbius mapping (albeit with different parameters), i.e. for any orbit of period m in the control subsystem (18a)–(18b) the mapping $x_n \to x_{n+m}$ is a Möbius mapping. Because this mapping is self-contained, it:

- or (i) has a pair of stable and unstable fixed points (within the base «sync region», where the rotation number is an integer);
- or (ii) by a smooth transformation $x \to y$ can be converted into a circle rotation $y_{n+m} = y_n + m\rho$, where ρ is the rotation number. This number depends monotonically on the parameters, which rules out the existence of higher order periodicity windows.

This feature of the Möbius map means that for any moving periodic orbit (t_n, s_n) in the equation 18c there is only one possible tangent (saddle-node) bifurcation separating modes (i) and (ii) . Figure 7 shows bifurcation curves corresponding to tangent bifurcations of periodic orbits with period ≤ 7 on the parameter plane (c, α) for fixed $\varepsilon = 0.4$ and $\mu = 0.1$.

It can be seen from Fig. 7 that for each value of the α parameter there is a range of positive values of the c parameter, $0 < c_1(\alpha, \mu, \varepsilon) \leq c \leq c_2(\alpha, \mu, \varepsilon)$, on which tangential bifurcations of periodic points of all possible periods occur. (The corresponding interval of negative values is c, $c_3(\alpha, \mu, \varepsilon) \leq c \leq c_4(\alpha, \mu, \varepsilon) < 0$). We will call these c parameter value ranges *transition regions*. Thus, the (18) system demonstrates three dynamic states depending on the value of the parameter c:

1. **Range of small $|c|$ (fig. 6a).** Separate attractor and repeller exist for $c_4(\alpha, \mu, \varepsilon) < c < c_1(\alpha, \mu, \varepsilon)$. Here the coordinate x on the attractor and repeller is a function depending on (t, s). This function is expected to be relatively smooth for large ε and non-smooth (fractal) for small ε. All other points of the phase space (with the exception of a set of measure zero) belong to the basin of the attractor (repeller, for a system in reverse time). The rotation number ρ is equal to zero here.

2. **Range of large $|c|$ (Fig. 6c).** Attractor and repeller intersect and do not have isolated periodic orbits for $c > c_2(\alpha, \varepsilon,\ mu)$ and $c < c_3(\alpha, \varepsilon, \mu)$. Thus, there are no hyperbolic sets for this range of parameters. The evolution of the variable x for each periodic orbit of the Anosov map is described by a superposition of the Möbius maps, which results in a Möbius map that is smoothly conjugate to a circle shift. This means that the complete system (18) does not have isolated periodic orbits.

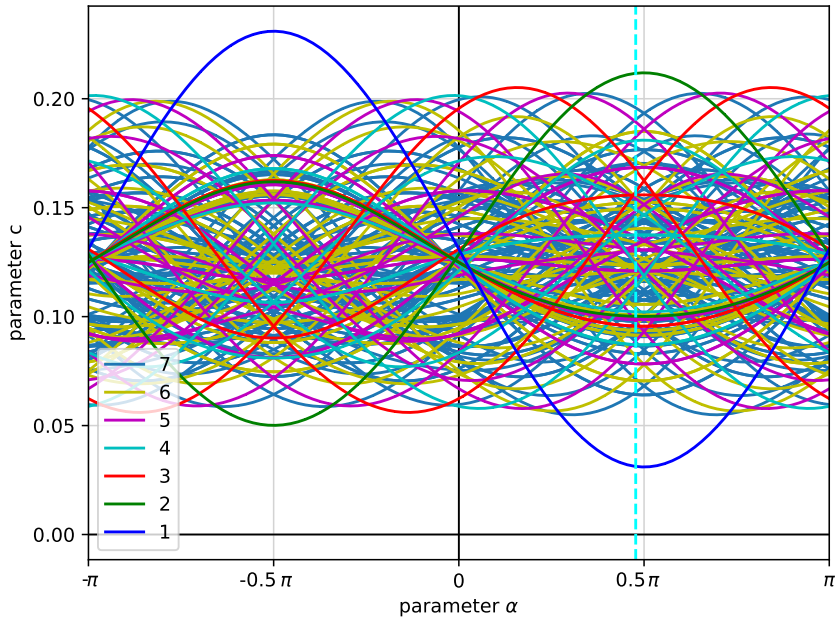

Рис. 7: Curves of tangent (saddle-node) bifurcations of the mapping (18) for all periodic orbits of the Anosov mapping with periods ≤ 7 (the curves for periodic orbits of the same period have the same color, see the legend in lower left corner), on the parameter plane (c, ε) for $\varepsilon = 0.4$ and $\mu = 0.1$. «Envelopes» of these curves define the boundary between modes 1 and 3 (small values of c) and between modes 2 and 3 (large values of c).

3. **The range of averages $|c|$ (Fig. 6b).** corresponds to the transition region. In these transition regions $c_1 \leq c \leq c_2$ and $c_3 \leq c \leq c_4$, some pairs of saddle periodic orbits have already disappeared as a result of the tangent bifurcation, and some still exist. Attractor and repeller overlap, but their measures are concentrated in different areas.

In the second part of Chapter 2, we construct a heterodimensional cycle in the region $c_1 \leq c \leq c_2$, i.e. a heteroclinic cycle connecting saddle periodic orbits inherited from the former attractor and repeller. For brevity, we call them *A-orbits* and *R-orbits*, respectively. These orbits have different dimensions of stable and unstable manifolds: A-orbits have two-dimensional stable and one-dimensional unstable manifolds (one stable and one unstable direction from the Anosov mapping (18a)–(18a) and one stable proper vector in the direction x), R-orbits have one-dimensional stable and two-dimensional unstable manifolds (here the eigenvector in the direction x is unstable).

A characteristic feature of mode 3 is the existence of heterodimensional cycles [22, 27, 28], consisting of pairs of heteroclinic trajectories connecting A-orbits with R-orbits: one of these trajectories lies in the transversal intersection of the two-dimensional manifolds of A-orbit and R-orbit , and the other one passes through a non-transversal (codimension 1) intersection of the one-dimensional manifolds of these orbits, see Fig. 8. In the second part of Chapter 2, we give numerical confirmation of the existence of such cycles. For simplicity, we restrict ourselves to the simplest case, when the A- and R-orbits have a period of two, and the pair of fixed points A_1 and R_1, which belonged to the attractor and the repeller, respectively, have already disappeared as a result of a tangent bifurcation.

In this case, it is more convenient to consider the second iteration of the mapping. Then the period two points A_2 and R_2 in the mapping (18) become fixed points. We denote the

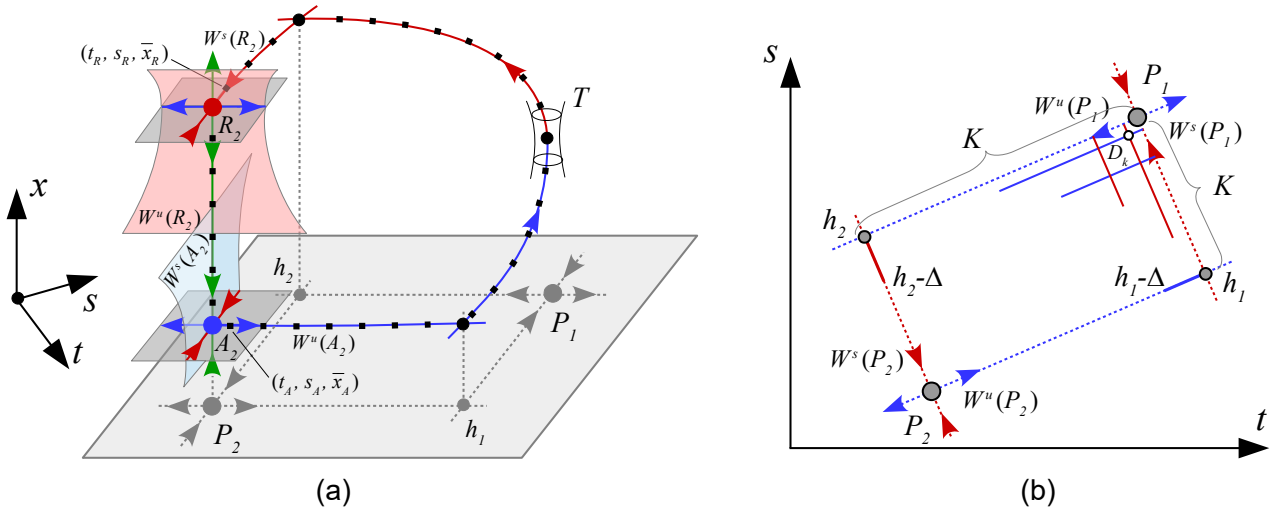

Рис. 8: (a) Illustration for the construction of a heterodimensional cycle connecting the points A_2 and R_2. Besides the points A_2 and R_2, this cycle also consists of two orbits (marked with black square dots). One (trivial) orbit belongs to the transversal intersection of the two-dimensional manifolds $W^s(A_2)$ and $W^u(R_2)$, only the variable x changes along this orbit (so it looks like a vertical line in the figure). Another (nontrivial) orbit passes through a nontransversal (codimension 1) intersection of the one-dimensional manifolds $W^u(A_2)$ and $W^s(R_2)$ inside the narrow tunnel T. Points P_1 and P_2 are a fixed point and a point of period 2 in the Anosov mapping (18a)–(18b); the heteroclinic points h_1 and h_2 belong to the intersection $W^u(P_2) \cap W^s(P_1)$ and $W^s(P_2) \cap W^u(P_1)$, respectively. (b) A heteroclinic cycle connecting the points P_1 and P_2 in the Anosov mapping (18a)–(18b). This construction is used to find the homoclinic orbit to the point P_2 in this mapping. This homoclinic orbit is then used as a control trajectory for the numerical construction of a heterodimensional cycle in the mapping (18).

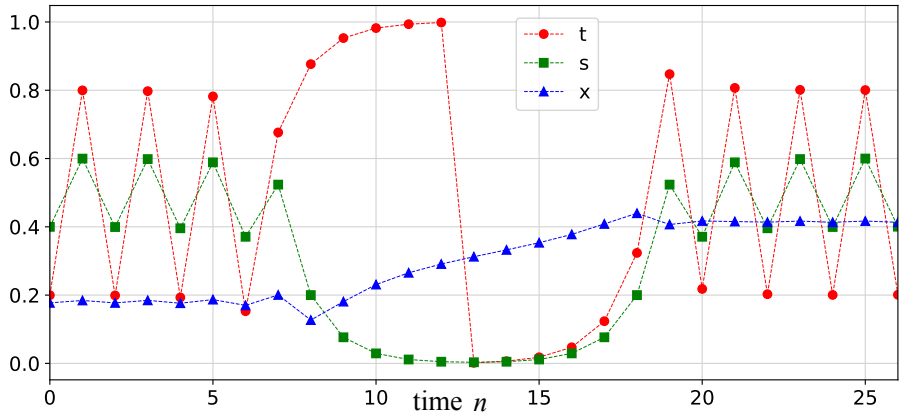

Рис. 9: Illustration for the construction of a heterodimensional cycle. Parameters: $\varepsilon = 0.4$, $\alpha = 1.5$, $\mu = 0.08$, $c = 0.07112495671202002$. It can be seen that, given the variables t and s (red and green markers), this trajectory is a homoclinic trajectory to the point of period two P_2 (for $n < 5$ and $n > 20$) passing near the fixed point $P_1 : (t, s) = (0, 0)$ (for $10 \lesssim n \lesssim 15$). While the trajectory (t, s) is near the fixed point P_1, the variable x (blue markers) changes from $x \approx 0.2$ (attractor position) to $x \approx 0.4$ (repeller position).

corresponding fixed point of the doubly applied Anosov map (18a)–(18b) by P_2, the fixed point of the Anosov map by P_1. The loop we'll build starts at A_2. Then the values of (t, s) become close to the fixed point P_1 and at these iterations the values of x move from the former attractor to the former repeller through a narrow tunnel (region T in Fig. 8a) located at the place where the fixed points A_1 and R_1 existed before the tangent bifurcation. After that, the trajectory approaches asymptotically close to R_2. This trajectory is marked in fig. 8a. Its numerical construction is shown in Fig. 9.

The algorithm for the numerical construction of a heterodimensional cycle consists of two stages. First, we compute the Anosov control trajectory (18a)–(18b) as a homoclinic trajectory for the point P_2 which comes very close to the fixed point P_1. At the next stage, we use this trajectory as a control trajectory in the Möbius mapping (18c) to construct a complete heteroclinic cycle connecting the points A_2 and R_2.

It is important to note that using the procedure described above, one can construct many different heterodimensional cycles (since there are (infinitely) many different homoclinic orbits to the point P_2 passing near the point P_1 in the Anosov map). However, this is not necessary, because according to the theory developed in [28], the existence of one heterodimensional cycle implies the existence of many such cycles in the neighborhood of the considered parameter values. Our calculations thus confirm that when an attractor and a repeller collide in the mapping (18), a heterodimensional dynamics arises. It is noteworthy that such a regime disappears when the «last» pair of periodic orbits disappears through a tangent bifurcation (i.e., the system goes into mode 2 according to the classification presented above). This is the specificity of the Möbius mapping, which can only have a couple of fixed points, but cannot have isolated periodic orbits of high periods.

2.3 Software package

The main part of the results of the dissertation research was obtained using numerical methods. To carry out the necessary numerical experiments, the dissertation student developed a software package. The functionality of the complex allows:

- calculate the Kantorovich-Rubinshtein-Wasserstein distance between the attractor and the repeller;
- compute relative Renyi dimensions and mutual singularities of attractor and repeller;
- build heterodimensional cycles for 3D systems showing the intersection of an attractor and a repeller.

To calculate the Kantorovich-Rubinstein-Wasserstein distance, we used two freely available software packages: «PyEMD: Earth mover's distance for Python» [40], which works on the basis of the algorithm described in Jensen's paper [41] and the package «CLP: COIN linear program code» [42], which implements direct methods for solving the simplex problem. The corresponding program codes were integrated into the structure of the dissertation's software package. Both of them gave the same results when calculating the Kantorovich-Rubinshtein-Wasserstein distance between the attractors and repellers of the maps (9), (10) and (11), as well as the flow (12).

A detailed description of all the necessary formulas for calculating the relative Renyi dimensions and mutual singularities is given in the second part of Chapter 2 of the thesis. Within the framework of the software package, the dissertation student developed numerical methods that implement the algorithm for calculating relative dimensions and mutual singularities using analytical formulas and numerical schemes described in the second part of Chapter 2.

Next, we give a more detailed description of the method for the numerical construction of a heterosized cycle.

- First, on the plane (t, s), find the intersection points h_1 and h_2 of the unstable manifold $W^u(P_2)$ with the stable manifold $W^s(P_1)$, and the unstable manifold $W^u(P_1)$ with the stable manifold $W^s(P_2)$, respectively, see fig. 8b. This is an easy task because all manifolds are straight lines. Thus, we construct two heteroclinic compounds $P_2 \to P_1$ and $P_1 \to P_2$.
- Then we find the homoclinic trajectory of the Anosov mapping (18a)–(18b) $P_2 \to P_2$ passing near the constructed heteroclinic cycles. To do this, on the unstable manifold $W^u(P_2)$, take a small segment $[h_1 - \Delta, h_1]$, where the point $h_1 - \Delta$ lies between the points P_2 and h_1. We iterate this segment forward in time (for example, apply K iterations) until the iteration of the point h_1 gets close enough to the point P_1. Similarly, on the stable manifold $W^s(P_2)$, take a small segment $[h_2 - \Delta, h_2]$, where the point $h_2 - \Delta$ lies between the points P_2 and h_2. We iterate it backwards in time (again K times) until iteration h_2 approaches P_1. This ensures that the corresponding images of the segments $[h_1 - \Delta, h_1]$ and $[h_2 - \Delta, h_2]$ intersect at some point D_k that is as close to P_1 as we want (increasing K, we can make the point D_k arbitrarily close to P_1).
- Iterations of the point D_k in the Anosov map (18a)–(18b) give a homoclinic orbit to the point P_2 which comes very close to the fixed point P_1 and thus spends a lot of time around this point. In what follows, we will use it as a driving force for the Möbius mapping (18c).

- In the next step, we find the point (t_A, s_A, x_A) on the unstable manifold $W^u(A_2)$ very close to the point A_2. To do this, take the point (t_A, s_A), which is very close to the point P_2 and at the same time belongs to the trajectory D_k. Then we select several values of x_i close to the x-coordinate of the point A_2 and iterate the points (t_A, s_A, x_i) back in time. The values of (t, s) converge to the point P_2, and the values of x either increase or decrease, except for those that belong to $W^u(A_2)$. Taking more values of x between neighboring points, which during these backward iterations pass along different branches (up and down) along the stable manifold $W^s(A_2)$ in the direction x, one can find the point (t_A, s_A, x_A) on an unstable manifold $W^u(A_2)$ with a given accuracy. In the same way we find the point (x_R, t_R, s_R) lying on the one-dimensional stable manifold of the point R_2.

- Finally, we iterate the points (t_A, s_A, x_A) and (x_R, t_R, s_R) forward and backward in time, respectively, until their (t, s)-coordinates reach the point D_k . Generally speaking, at this point the resulting coordinates $\overline{x}_A$ and $\overline{x}_R$ do not match. However, by varying one of the parameters in the (18) mapping (we varied the c parameter), we can find the value at which $\overline{x}_A = \overline{x}_B$. This completes the construction of a heteroclinic connection between the one-dimensional manifolds $W^u(A_2)$ and $W^s(R_2)$ of the desired heterodimensional cycle.

- Note that there always exists an intersection of the two-dimensional manifolds $W^u(R_2)$ and $W^s(A_2)$, which provides the second heteroclinic connection between the points R_2 and A_2. Thus, the described procedure gives numerical confirmation of the existence of a heterosized ring.

References

[1] Topaj D., Pikovsky A. Reversibility vs. synchronization in oscillator lattices //Physica D: Nonlinear Phenomena. – 2002. – Т. 170. – №. 2. – С. 118-130.

[2] Gonchenko S. V., Turaev D. V., Shilnikov L. P. On Newhouse domains of two-dimensional diffeomorphisms which are close to a diffeomorphism with a structurally unstable heteroclinic cycle //Proc. Steklov Inst. Math. – 1997. – Т. 216. – С. 70-118.

[3] Lamb J. S. W., Stenkin O. V. Newhouse regions for reversible systems with infinitely many stable, unstable and elliptic periodic orbits //Nonlinearity. – 2004. – Т. 17. – №. 4. – С. 1217.

[4] Delshams A. et al. Abundance of attracting, repelling and elliptic periodic orbits in two-dimensional reversible maps //Nonlinearity. – 2012. – Т. 26. – №. 1. – С. 1.

[5] Gonchenko S. V. Reversible mixed dynamics: A concept and examples //Discontinuity, Nonlinearity, and Complexity. – 2016. – Т. 5. – №. 4. – С. 365-374.

[6] Gonchenko S. V., Turaev D. V. On three types of dynamics and the notion of attractor //Proceedings of the Steklov Institute of Mathematics. – 2017. – Т. 297. – С. 116-137.

[7] Kazakov A. O. Strange attractors and mixed dynamics in the problem of an unbalanced rubber ball rolling on a plane //Regular and Chaotic Dynamics. – 2013. – Т. 18. – №. 5. – С. 508-520.

[8] Gonchenko A. S., Gonchenko S. V., Kazakov A. O. Richness of chaotic dynamics in nonholonomic models of a Celtic stone //Regular and Chaotic Dynamics. – 2013. – Т. 18. – С. 521-538.

[9] Gonchenko S. V., Gonchenko A. S., Kazakov A. O. Three types of attractors and mixed dynamics of nonholonomic models of rigid body motion //Proceedings of the Steklov Institute of Mathematics. – 2020. – Т. 308. – С. 125-140.

[10] Bizyaev I. A., Mamaev I. S. Separatrix splitting and nonintegrability in the nonholonomic rolling of a generalized Chaplygin sphere //International Journal of Non-Linear Mechanics. – 2020. – Т. 126. – С. 103550.

[11] Kuznetsov S. P., Kruglov V. P., Borisov A. V. Chaplygin sleigh in the quadratic potential field //Europhysics Letters. – 2020. – Т. 132. – №. 2. – С. 20008.

[12] Kazakov A. Merger of a Henon-like attractor with a Henon-like repeller in a model of vortex dynamics<? A3B2 show [editpick]?> //Chaos: An Interdisciplinary Journal of Nonlinear Science. – 2020. – Т. 30. – №. 1. – С. 011105.

[13] Emelianova A. A., Nekorkin V. I. On the intersection of a chaotic attractor and a chaotic repeller in the system of two adaptively coupled phase oscillators //Chaos: An Interdisciplinary Journal of Nonlinear Science. – 2019. – Т. 29. – №. 11. – С. 111102.

[14] Emelianova A. A., Nekorkin V. I. The third type of chaos in a system of two adaptively coupled phase oscillators //Chaos: An Interdisciplinary Journal of Nonlinear Science. – 2020. – Т. 30. – №. 5. – С. 051105.

[15] Emelianova A. A., Nekorkin V. I. Emergence and synchronization of a reversible core in a system of forced adaptively coupled Kuramoto oscillators //Chaos: An Interdisciplinary Journal of Nonlinear Science. – 2021. – Т. 31. – №. 3. – С. 033102.

[16] Gonchenko A. S. et al. On the phenomenon of mixed dynamics in Pikovsky–Topaj system of coupled rotators //Physica D: Nonlinear Phenomena. – 2017. – Т. 350. – С. 45-57.

[17] Kazakov A. O. On the appearance of mixed dynamics as a result of collision of strange attractors and repellers in reversible systems //Radiophysics and Quantum Electronics. – 2019. – Т. 61. – С. 650-658.

[18] Bizyaev I. A., Borisov A. V., Kazakov A. O. Dynamics of the Suslov problem in a gravitational field: Reversal and strange attractors //Regular and Chaotic Dynamics. – 2015. – Т. 20. – С. 605-626.

[19] Turaev D. A criterion for mixed dynamics in two-dimensional reversible maps<? A3B2 show [editpick]?> //Chaos: An Interdisciplinary Journal of Nonlinear Science. – 2021. – Т. 31. – №. 4. – С. 043133.

[20] Muskulus M., Verduyn-Lunel S. Wasserstein distances in the analysis of time series and dynamical systems //Physica D: Nonlinear Phenomena. – 2011. – Т. 240. – №. 1. – С. 45-58.

[21] Pikovsky A. et al. Attractor-repeller collision and eyelet intermittency at the transition to phase synchronization //Physical review letters. – 1997. – Т. 79. – №. 1. – С. 47.

[22] Bonatti C., Diaz L. J. Persistent nonhyperbolic transitive diffeomorphisms //Annals of Mathematics. – 1996. – Т. 143. – №. 2. – С. 357-396.

[23] Abraham R., Smale S. Nongenericity of Ω-stability //The Collected Papers of Stephen Smale: Volume 2. – 2000. – С. 735-738.

[24] Diaz L. J., Rocha J. Nonconnected heterodimensional cycles: bifurcation and stability //Nonlinearity. – 1992. – Т. 5. – №. 6. – С. 1315.

[25] Diaz L. J. Robust nonhyperbolic dynamics and heterodimensional cycles //Ergodic Theory and Dynamical Systems. – 1995. – Т. 15. – №. 2. – С. 291-315.

[26] Diaz L. J. Persistence of cycles and nonhyperbolic dynamics at heteroclinic bifurcations //Nonlinearity. – 1995. – Т. 8. – №. 5. – С. 693.

[27] Bonatti C., Diaz L. J. Robust heterodimensional cycles and-generic dynamics //Journal of the Institute of Mathematics of Jussieu. – 2008. – Т. 7. – №. 3. – С. 469-525.

[28] Li D., Turaev D. Persistence of heterodimensional cycles //arXiv preprint arXiv:2105.03739. – 2021.

[29] Hittmeyer S. et al. Existence of blenders in a Henon-like family: Geometric insights from invariant manifold computations //Nonlinearity. – 2018. – T. 31. – №. 10. – C. R239.

[30] Hittmeyer S. et al. How to identify a hyperbolic set as a blender //Discrete and Continuous Dynamical Systems. – 2020. – T. 40. – №. 12. – C. 6815-6836.

[31] Hammerlindl A. et al. Determining the global manifold structure of a continuous-time heterodimensional cycle //Journal of Computational Dynamics. – 2022. – T. 9. – №. 3. – C. 393-419.

[32] Katok A., Hasselblatt B. Introduction to the modern theory of dynamical systems. – Cambridge university press, 1995. – №. 54.

[33] Chirikov B., Shepelyansky D. Chirikov standard map //Scholarpedia. – 2008. – T. 3. – №. 3. – C. 3550.

[34] Duarte P. Plenty of elliptic islands for the standard family of area preserving maps //Annales de l'Institut Henri Poincare C, Analyse non lineaire. – No longer published by Elsevier, 1994. – T. 11. – №. 4. – C. 359-409.

[35] Cornfeld I. P., Fomin S. V., Sinai Y. G. Ergodic theory. – Springer Science & Business Media, 2012. – T. 245.

[36] Marvel S. A., Mirollo R. E., Strogatz S. H. Identical phase oscillators with global sinusoidal coupling evolve by Mobius group action //Chaos: An Interdisciplinary Journal of Nonlinear Science. – 2009. – T. 19. – №. 4. – C. 043104.

[37] Gong C. C., Toenjes R., Pikovsky A. Coupled Mobius maps as a tool to model Kuramoto phase synchronization //Physical Review E. – 2020. – T. 102. – №. 2. – C. 022206.

[38] Grassberger P., Procaccia I. Characterization of strange attractors //Physical review letters. – 1983. – T. 50. – №. 5. – C. 346.

[39] Lai Y. C., Tél T. Transient chaos: complex dynamics on finite time scales. – Springer Science & Business Media, 2011. – T. 173.

[40] Doran G. PyEMD: Earth mover's distance for Python. – 2014.

[41] P. Jensen. Operation research methods, 1999. [Online; accessed May 2020].

[42] Forrest J., de la Nuez D., Lougee-Heimer R. CLP user guide, 2004 //Software available at http://www.coin-or.org/Clp/index.html. – 2010.